Atmos. Chem. Phys. Discuss., 12, 2025–2056, 2012
www.atmos-chem-phys-discuss.net/12/2025/2012/
doi:10.5194/acpd-12-2025-2012

Atmospheric Chemistry and Physics Discussions

Can a global model reproduce observed trends in summertime surface ozone levels?

S. Koumoutsaris[1,*] **and I. Bey**[2]

[1]International Space Science Institute, Bern, Switzerland
[2]Center for Climate Systems Modeling, ETH Zurich, Zurich, Switzerland
[*]now at: Risk Management Solutions, EC3R 8NB, London, UK

Received: 23 December 2011 – Accepted: 3 January 2012 – Published: 20 January 2012

Correspondence to: S. Koumoutsaris (koumoutsaris@issibern.ch)

Published by Copernicus Publications on behalf of the European Geosciences Union.

Abstract

Quantifying trends in surface ozone concentrations are critical for assessing pollution control strategies. Here we use observations and results from a global chemical transport model to examine the trends (1991–2005) in daily maximum 8-hour average concentrations in summertime surface ozone at rural sites in Europe and the United States. We find a decrease in observed ozone concentrations at the high end of the probability distribution at many of the sites in both regions. The model attributes these trends to a decrease in local anthropogenic ozone precursors, although simulated decreasing trends are overestimated in comparison with observed ones. The low end of observed distribution show small upward trends over Europe and the western US and downward trends in Eastern US. The model cannot reproduce these observed trends, especially over Europe and the western US. In particular, simulated changes between the low and high end of the distributions in these two regions are not significant. Sensitivity simulations indicate that emissions from far away source regions do not affect significantly ozone trends at both ends of the distribution. This is in contrast with previously available results, which indicated that increasing ozone trends at the low percentiles may reflect an increase in ozone background associated with increasing remote sources of ozone precursors. Possible reasons for discrepancies between observed and simulated trends are discussed.

1 Introduction

Quantifying surface background ozone concentrations and associated trends is critical for understanding the processes influencing tropospheric ozone (O_3) budget and assess pollution control strategies (Lin et al., 2000; Vingarzan, 2004). Long-term trends in tropospheric O_3 are however difficult to infer due to their large natural variability and to the scarcity of long records of reliable ozone measurements (Staehelin and Weiss, 2001; Oltmans et al., 2006; IPCC, 2007). Even the sign and magnitude of long-term

ACPD
12, 2025–2056, 2012

tropospheric O_3 trends (as well as the causes of these changes) differ significantly between nearby locations (Oltmans et al., 2006). Although current trends are not geographically uniform, recent studies report declining trends in O_3 concentrations at urban sites and at sites downwind of urban centers in North America and Europe (Vingarzan, 2004, and references therein). These declines are more evident in the high end of the distribution and appear to be associated with declining local ozone precursor emissions (Bronnimann et al., 2002; Vingarzan, 2004; Jonson et al., 2006). In contrast, increasing trends are often seen for values at the mid and low end of the distribution and are likely related with increasing trends in background (i.e. not directly due to local emissions) ozone concentations (Lin et al., 2000; Jonson et al., 2006). The origin of this increase in ozone background is still unclear (Bronnimann et al., 2002; Jonson et al., 2006) but some of the plausible factors include changes in ozone precursor emissions with subsequent long range transport, change in stratospheric-tropospheric exchange, and global rise in methane levels (Vingarzan, 2004; Cooper et al., 2010).

The objectives of this study are to assess the ability of a state-of-the-art global chemical transport model to reproduce observed trends in surface ozone and to quantify the contribution of O_3 precursor emissions from distant sources over Europe and North America. We focus over the summer season, where sunshine drives O_3 levels above the air pollution regulations defined by environmental protection agencies. We compare the observed and simulated change in the probability distribution of the daily maximum 8-hour average summer O_3 concentration for a period from 1991 to 2005. Hourly observations from the European Monitoring and Evaluation Programme (EMEP) (EMEP, 2008), the World Data Centre for Greenhouse Gases (WDCGG) (WMO, 2008), and the Clean Air Status and Trends Network (CASTNET) (EPA, 2007) were used, conjointly with results from a 15-year simulation performed with the global chemistry transport model GEOS-Chem (Koumoutsaris et al., 2008). A description of the model, emission inventory and simulations used in this study is given in Sect. 2. The methods used to compute the observed and simulated trends are presented in Sect. 3. Results for Europe and United States (US) are shown in Sect. 4 and are further discussed in

ACPD
12, 2025–2056, 2012

Sect. 5.

2 The GEOS-Chem model

We use the GEOS-CHEM model, a global chemical-transport model driven by assimilated meteorological data from the Data Assimilation Office NASA Global Modeling and Assimilation Office of NASA (Bey et al., 2001b). The work shown here employed the version v7-03-06 of GEOS-CHEM (http://acmg.seas.harvard.edu/geos/) that is driven by the GEOS-4 assimilated meteorological observations. The GEOS-4 dataset has a temporal resolution of 6 h (3 h for surface variables and mixing depths), a horizontal resolution of 1°×1.25°, and 55 layers in the vertical from the surface up to 0.01 hPa. We degrade the horizontal resolution to 2°×2.5° and 30 layers in the vertical. A detailed description on the model configuration used here can be found in Koumoutsaris et al. (2008), except for O_3 precursor emissions described below.

2.1 Ozone precursor emissions used in this study

Anthropogenic emissions of trace gases are based on an emission inventory for 1985 described by Wang et al. (1998b), that includes NO_x emissions from the Global Emission Inventory Activity (GEIA) (Benkovitz et al., 1996), non-methane hydrocarbon (NMHC) emissions from Piccot et al. (1992), and CO emissions from Duncan et al. (2007), scaled until 1998, as described in Bey et al. (2001a). We further implemented interannual varying emissions over the most important anthropogenic source regions. More precisely, we implemented the European Monitoring and Evaluation Program (EMEP) Expert emissions (Vestreng et al., 2006) over the European continent. During the period from 1990 to 2005, EMEP emissions show a strong decrease over Europe (35° N–65° N, 10° W–40° E), as shown in Fig. 1 (−1.6 % per year for NO_x and −2.7 % per year for CO). Trends in emissions for certain volatile organic compounds (VOCs) (propene, butane, ethane, methyl-ethyl-ketone and acetaldehyde) were also

ACPD
12, 2025–2056, 2012

implemented. For the US, we use the Environmental Protection Agency (EPA) National Emissions Inventory (NEI) 1999 v.1 inventory (NEI99, http://www.epa.gov/ttn/chief/net/1999inventory.html, with some modifications as described in Hudman et al. (2007), which we scale with the NEI Emissions trends data provided by the EPA (EPA, 2007). Notice however that the scaling is applied uniformally all over the US and to all VOCs. Emissions from Canada and Mexico are not varying after 1998, but they account together for less than 10 % of the US emissions. Figure 1 shows the year-to-year variation in NO_x and CO anthropogenic emissions over North America (125° W–60° W, 15° N–55° N) for the period from 1990 to 2005. The trends in NO_x and CO emissions are −1 % and −1.7 % per year, respectively. For Asia, we implemented the Regional Emission Inventory in Asia (REAS) (Ohara et al., 2007) for NO_x, CO and VOCs (propene, propane, butane, ethane, methyl-ethyl-ketone). Data are available from 1990 to 2005, however, the last two years (2004 and 2005) are "predictions" (Ohara et al., 2007) and show lower interannual variability. The interannual variability in emissions for South Asia (50° E–95° E, 5° N–35° N) and East Asia (95° W–160° W, 15° N–50° N) is shown in Figure 1 (bottom panels). Anthropogenic emissions strongly increase in East Asia from 1990 to 2005, especially for NO_x (5.8 % per year). The decrease of CO emissions from 1995 to 2005 is due to a reduction in consumption of coal and biofuel in the domestic sector during this period. This lead to a smaller CO trend of 1 % per year. South Asian emissions also increase significantly during our study period (3.2 % per year for NO_x and 1.5 % per year for CO). Ship emissions are accounted in the model in the eastern Atlantic and the Indian ocean as part of the EMEP and REAS inventories, respectively. Even though ship emissions are taken into account only partially in the model, recent studies support that the effects of international shipping over the European continent are rather small (Jonson et al., 2006). Finally, we have also implemented a +3 % annual increment of global NO_x aircraft emissions (0.5 TgN in 1992) following IPCC (1999) and EPA (2000) reports.

Soil NO_x emissions (~5.9 TgN per year) are calculated according to the Yienger and Levy (1995) algorithm with the canopy reduction factor described in Wang et al.

ACPD
12, 2025–2056, 2012

(1998a). Biomass burning emissions are derived from an inventory of the total annual biomass burned described in Lobert et al. (1999) and Duncan et al. (2003). Annual biomass burned is converted to NO_x emissions by applying emission factors, providing a climatological inventory for biomass burning emissions, as described in Duncan et al. (2003). Interannual variations are further accounted for using the TOMS Aerosol Index product (Torres et al., 1998; Herman et al., 1997; Hsu et al., 1996) from January to July 1996 following Duncan et al. (2003) and the Advanced Along Track Scanning radiometer (AATSR) active fire dataset (Arino and Melinotte, 1995) from August 1996 to 2005 following Generoso et al. (2003) with slight improvements as described in Koumoutsaris et al. (2008). The global annual biomass burning emissions range from 5 to 8 TgN during our study period. Emissions of NO_x from lightning (~6 TgN per year) are linked to deep convection following the parametrization of Price and Rind (1992) with vertical profiles from Pickering et al. (1998) as implemented by Wang et al. (1998b).

2.2 Simulations

We first performed a 15-year control simulation (labelled "S0") from January 1991 to December 2005. We then carried out four sensitivity simulations from 2001 to 2005 with anthropogenic emissions of specific geopolitical regions – including Europe ("SEur"), North America ("SNAm"), South Asia ("SSAs"), and East Asia ("SEAs") – set to the year 1990 (see also Table 1). An additional sensitivity simulation ("SXEur") was performed with anthropogenic emissions over North America, South and East Asia, and methane concentrations fixed to the 1990 levels to assess their combined impact in European ozone levels. Finally, we performed another simulation ("SMet") for the period 2001–2005 (that is emissions from 2001–2005) but with meteorology from 1991–1995, to examine the impact of changing meteorology and climate over the 10-year period.

ACPD
12, 2025–2056, 2012

3 Method

We use hourly O_3 data available from the EMEP, WDCGG, and CASTNET databases to compute the daily summer (June–July–August) maximum 8-h average O_3 concentration (according to the EPA regulations (EPA, 1998) and named as "8 h-max O_3", hereafter) at several sites over Europe and the US. We only use the sites with at least 30 days of data in summer for each year from 1991 to 2005. There are 44 sites in Europe and 38 sites in the US that meet these criteria. For each site, we examine the linear trends of several percentile populations, as shown for example for Illmitz (Austria) in Fig. 2. The location of the sites and the observed and simulated trends at the 5th and 95th percentile are presented in Figs. 3 and 4 for Europe and US, respectively.

We next compute the cumulative probability distribution (CPD) of the 8 h-max O_3 concentrations aggregated over the ensembles of stations for Europe (Fig. 5) and for US (Fig. 6). We compare the distributions at the beggining and at the end of the record, 1991–1994 vs. 2001–2005 for both observations and model. We use 5-year periods in order to reduce the effect of interannual variability associated with meteorology. However, we exclude the year 2003 which has been particular anomalous (heat wave) over Europe (Schär et al., 2004). The statistical significance of the difference between the two distributions is determined by comparing the populations of several percentiles (5th, 10th, 20th, etc.) with the two-sided Kolmogorov-Smirnov statistic test following Lin et al. (2000).

4 Observed and simulated ozone trends

4.1 Europe

In a previous study, we have discussed the ability of the GEOS-Chem model to simulate the interannual variation in O_3 concentrations at the northern mid-latitudes (Koumoutsaris et al., 2008). Even though the model is able to capture some of the large

ACPD
12, 2025–2056, 2012

interannual variations (e.g. the 1998–1999 anomaly), not all features were well represented in several sites, which is probably related to a poor representation of stratospheric chemistry and dynamics (Koumoutsaris et al., 2008). The model's ability in representing the surface O_3 summer-mean is shown in Table 2 which compares the simulated summer-mean with observations for the period 1991 to 2005 at different percentiles. In the majority of the European sites, the agreement at the lower percentiles is very low with almost 50 % of the sites presenting correlation coefficients lower than 0.3. The model reproduces better the summer O_3 interannual variation at the high percentiles. More than 55 % of the sites show a correlation larger or equal to 0.7 at the 95th percentile. The fact that the model's performance decreases in the majority of the sites at the low end of the distribution, where O_3 is more inflenced by background concentrations, is reflected in the representation of the trends and will be discussed in more details in the following sections. The mean bias between the model and the observations is relatively low with best performace at the median concentrations. The model (under-) over-estimate of O_3 concentrations at the (high) low end of the distribution may be due at least to some extent to the model resolution which is too coarse to capture the very high and the very low events.

The observed and simulated summer O_3 trends at the 95th and 5th percentiles are shown in Fig. 3. One important point to note is that the observed 8 h-max O_3 trends in Europe show large variability even between nearby sites. For example, the observed O_3 trends at the 5th percentile range between 1.52 ± 0.57 ppbv year^{-1} and 0.28 ± 0.39 ppbv year^{-1} at the two nearby stations of Langerbrügge (10.75° E, 52.8° N) and Waldhof (10.77° E, 52.8° N) in Germany. Despite these apparent inconsistencies, we find decreasing (increasing) concentrations at the high (low) end of the distribution, respectively (Fig. 5). Note that we only computed trends throughout the period 1991 to 2005, while different values may be found if one considers shorter periods (Logan et al., 2010).

ACPD
12, 2025–2056, 2012

4.1.1 Low percentiles

Observations show very large spatial variability across Europe. We find positive trends at several sites, although statistically significant only at a few of them (Fig. 3). The increases in the observed 8 h-max O_3 concentrations in the low end of the distribution has been suggested to be related to an increase in background O_3 concentrations, especially at high mountain sites, which are considered more representative for background conditions (Cristofanelli and Bonasoni, 2009). Nevertheless, even between high mountain sites there are differences in the observed trends (Fig. 3) that may be related to e.g., local wind systems (Zellweger et al., 2000). Cui et al. (2011) found that summer convective boundary layer can reach the altitudes of Jungfraujoch during high-pressure conditions, resulting in high ozone concentrations in 2003; This could balance the effect of a decrease in European precursor emissions. The aggregated results of the observations over the ensemble of the stations (29 stations in total, excluding the ones affected by titration: see below) are shown in the left panel of Fig. 5. The low tail of the observed CPD shows small but insignificant (at the 0.05 level) changes between 1991–1994 and 2001–2005 in the summer 8 h-max O_3 levels. The change in the CPD is not significant even if we consider only the high altitude sites of central Europe (not shown), even though there is a clear qualitative change in the observed O_3 trends between the low and high percentiles.

In contrast to the observations, the model simulates upward trends at most of the sites in the northwestern and central part of Europe, in UK and in Germany (Fig. 3), which however are due to titration effects as a response to the reduction in NO_x emissions over high polluted regions (Simpson, 1995; Jonson et al., 2006). The titration effect can be estimated by examining the chemical regime (i.e., the so called "O_3-NO_x-VOC" sensitivity) at each site, which requires concurrent observations of the atmospheric nitrogen compounds. As these data are not available, we use the ratio between the simulated 8 h-max O_3 and the simulated hourly total reactive nitrogen ($NO_y = NO + NO_2 + NO_3 + HNO_2 + HNO_3$) over each station as our NO_x-VOC indicator

ACPD
12, 2025–2056, 2012

(Sillman and He, 2002). A site with a ratio lower than 5 during several days in summer indicates a "VOC-sensitive" character. This occurs at most of the northwestern stations of Europe (3 Belgium sites, 3 northern German sites, and 9 sites in the United Kingdom: all except the ones in Ireland). Because of its coarse resolution, the model probably fails to represent correctly the "rural" character of these sites. Note however that the titration effect may affect some of the observed distributions as well, since even though the sites may be designated as background "rural", they can be subject to anthropogenic pollution under the influence of specific synoptic patterns (Vingarzan, 2004). However, due to lack of concurrent long-term observations of atmospheric nitrogen compounds, it is not possible to test for titration effect in the observed distributions. Titration by NO could be a problem when interpreting long-term trends in the lower end of the probability distribution (Lin et al., 2000), and thus we exclude these 15 "VOC-sensitive" sites from the dataset for our analysis.

The model has difficulties in reproducing the observed trends at the rest of the sites, where it shows mostly decreasing O_3 concentrations in comparison to the observed small but upward trends. This indicates performance issues at the low end of the distribution. We find insignificant contribution from distant sources (Asia and North America) to the low O_3 levels. Possible reasons for the discrepancies between model and observations are discussed in Sect. 5.

4.1.2 High percentiles

At the high end of the distribution (top panels in Fig. 3), observations show declining 8 h-max O_3 concentrations at several sites, although only few of them (8 among 44) are significant at the 0.05 level. In addition, upward trends are seen over some stations of central Europe e.g., Jungfraujoch in Switzerland and Vezin in Germany. The only station with statistically significant upward trend is Jungfraujoch (0.69 ± 0.58 ppbv year^{-1} at the 95th percentile) which is located at 3758 m a.s.l. The model, on the other hand, shows significant downward trends in most of the European sites.

ACPD
12, 2025–2056, 2012

Above ~44 ppbv, the observations show lower concentrations in 2001–2005 in comparison to 1991–1995 (Fig. 5). The difference between the two distributions is significant to the 0.05 level above the 40th percentile (not shown). The model (right panel of Fig. 5) shows similar behaviour, but the decrease in surface 8 h-max O_3 concentrations between the two periods is overestimated by 4–5 ppbv. Sensitivity model simulations indicate that downward trends at the high end of the distribution is mostly related to the decrease in European emissions during this period (Fig. 5) due to pollution control measures (EEA, 2007). Meteorology is also found to contribute significantly to the decrease in surface O_3 according to the modeling results (simulation SMet). We performed several additional sensitivity simulations to examine the influence of individual parameters, such as temperature, clouds, UV radiation, horizontal and vertical winds, and planetary boundary layer height. None of the O_3 distributions obtained from these simulations was significantly different from the control run, which could reflect that the influence of meteorology results from a combination of different parameters. The influence of long-range transport of anthropogenic emissions from sources outside Europe (e.g., North America or Asia) in summer is found to be negligible in the model for the sites we examined.

4.2 United States

The correlation between observed and modeled 8 h-max O_3 is somewhat better at the US sites (Table 2) in comparison to Europe, but the mean bias is much higher, especially at the low percentiles. Similarly to Europe, the correlation is low at most of the sites at the lower percentiles, indicating performance issues when O_3 levels are strongly influenced by background concentrations. In a recent study, Hogrefe et al. (2011) find a marked disagreement between observed and simulated O_3 trends for the lower percentiles over the North-Eastern US, which were found to be particularly sensitive to the choise of lateral boundary conditions (and thus long-range transport of pollutants) of their regional model. As reported previously for Europe, the model represents much better the high percentiles both in terms of interannual variation and

ACPD
12, 2025–2056, 2012

bias in all investigated sites. We find a decrease in the correlation at the 95th percentile at the US sites (both in the eastern and the western part: not shown), but we could not find any reasonable explanation.

Figure 4 shows the 8 h-max O_3 trends at the 5th and 95th percentile for both observations and the model for the CASTNET stations. A clear longitudinal difference is evident in the observations. Increasing trends are found at the western mountainous sites, in contrast to the eastern sites where a strong decrease is seen in most cases. The model reproduces the contrasted geographical features in the trends, although it underestimates significantly their magnitude in the western part. Due to the large differences between these two regions, we discuss separately the western (east of 100° W) and the eastern (west of 100° W) sites.

Almost all the eastern sites (all of them being at low altitudes) show decreasing trends (significant at the 0.05 level) in the observations at both high and low observed percentiles. The decrease in the peak O_3 concentrations is more pronounced in the north-eastern part of the region, a power plant dominated NO_x source region, where emission controls have been succesfully implemented (Kim et al., 2006; Frost et al., 2006). The model is not able to capture these trends since the trends in the model emission inventory have been applied all over the US uniformally (see Sect. 2). The decline in local emissions is responsible for the decreasing O_3 trends according to the model sensitivity simulations (simulation SNAm, Fig. 6). Negligible influence was found from sources in Asia or Europe.

In the western part, we found significant (at the 0.05 level) upward trends in the observed 8 h-max O_3 concentrations, which is larger at the low percentiles. The model underestimates significantly these trends (Fig. 4) and finds no significant difference between the two periods (Fig. 6). Furthermore, we did not find any statistically significant differences between the sensitivity simulations and the control run. Notice that 5 among 6 of the western US sites are in mountain regions (above 1500m a.s.l.) and thus more sensitive to Asian pollution because of their exposure to the free troposphere. We further discuss this issue in the following section.

ACPD
12, 2025–2056, 2012

5 Discussion

We have shown in previous sections that the GEOS-Chem model has difficulty in simulating the trends in O_3 concentrations, in particular at the low percentiles and at mountain sites in both Europe and US. These trends probably reflect changes in background ozone concentrations that are not captured by the model. There are several processes that have been suggested to explain this trends, including long-range transport from Asia (Lin et al., 2000; Fiore et al., 2002; Naja et al., 2003; Jaffe et al., 2003), change in methane concentrations (Fiore et al., 2009), and changes in stratospheric ozone (Ordóñez et al., 2007). In the following, we discuss in detail each of these processes in our model in an attempt to uncover the possible reasons of the model inconsistency with the observations.

5.1 Long-range transport from Asia

In summer, the transport from Asia occurs predominatly in warm conveyor belts of midlatitude cyclones, deep convection, and in typhoons (Liang et al., 2007). A significant fraction of the summertime ouflow is also transported westwards to the Middle East and may affect Europe (Liu et al., 2003; Auvray and Bey, 2005). Xu et al. (2008) and Ohara et al. (2008) found increasing O_3 trends in all seasons at a background station in eastern China and in Japan, respectively, and attributed those to the increase in Chinese NO_x emissions. The only East Asian site in the WDCGG data that meets our criteria (defined in Sect. 4.1) is Ryori, in Japan, where the observations show upward trends from 1991 to 2005 in surface 8 h-max O_3 summer concentrations at all percentiles of the distribution (not shown). The model once again underestimates the observed trends. We find similar results for carbon monoxide concentrations (CO). We computed CO trends from monthly mean data from WDCGG and the model standard simulation (S0) (Fig. 7). The model underestimates the annual summer (JJA) trends in CO over the same period (1991 to 2005), at several sites over the globe. The model's inability to capture the trends in the long-range transport events over the Pacific may

ACPD
12, 2025–2056, 2012

be related to

a. An underestimate of Asian O_3 precursor emission trends. Indeed, it has been suggested that the REAS emission inventory used in our study for Asia underestimates Asian NO_x emissions and trends (Kurokawa et al., 2009; Uno et al., 2007). More precisely, Uno et al. (2007) compared the NO_2 columns from satellite observations with the results from the CMAQ regional model fed with the REAS emission inventory and concluded that REAS most likely underestimates not only the magnitude over polluted industrial regions in Asia but also the rapid growth of the Chinese emissions during the period from 1996 to 2002. Kurokawa et al. (2009) also found that the REAS emissions underestimate the rate of increase in NO_x emissions in July from 1996 to 2002, when compared with optimized emissions derived from data assimilation of satellite observations.

b. A change in the Asian outflow and the associated chemical processes during the studied period that is not captured by the model. Our results show that the location or intensity of the Asian O_3 transport has not significantly changed over the studied period. The fixed meteorology (SMet) simulation shows little influence in O_3 trends at the western US sites (not shown). However, several studies have indicated that the model has some problems in simulating the chemical processes inside the transport plumes. Liang et al. (2007) for example, found that the GEOS-Chem model captures the timing and location of the Asian plumes, but it significantly underestimates the magnitude of observed enhancements in CO, O_3, PAN and NO_x, during the INTEX-A campaing (July to August 2004). Zhang et al. (2008) also find 15 % lower CO over the Pacific (INTEX-B aircraft campain) in spring for GEOS-Chem, which attribute to an overestimate in hydroxyl radical (OH) in the model. At this stage, it is unclear to what extent these model biases can affect the simulated tropospheric O_3 trends.

ACPD
12, 2025–2056, 2012

5.2 Change in methane concentrations

Methane (CH_4), besides being an important greenhouse gas, is also a known major source of the background tropospheric O_3 concentrations. Our model uses annual and latitudinally prescribed observed CH_4 concentrations. When CH_4 concentrations are kept fixed to the 1990 levels, we find negligible contribution of changing CH_4 concentrations on the 8 h-max O_3 summer trends.

5.3 Changes in stratospheric ozone

Another plausible factor for the increase in the background O_3 levels is the stratosphere-troposphere exchange. There are indications that O_3 at mountain tops in Europe increase due to stratospheric input (Ordóñez et al., 2007; Tarasova et al., 2009). Furthermore, the transport of Asian pollution in the upper troposphere over the Pacific has been shown to be subject to mixing with lower stratospheric air in summertime (Liang et al., 2007). Hudman et al. (2004) found that the model underesimates the stratospheric contribution to O_3 in the middle troposphere in spring 2002 over the Pacific. Moreover, Koumoutsaris et al. (2008) have demonstrated the difficulty of the model in representing the interannual variability at several sites in the northern mid-latitudes, that are likely affected by stratospheric chemistry and dynamics. Stratosphere-troposphere exchange is a major source of O_3 in the troposphere and is expected to play an even more important role in the future, since an increase in the net transport of O_3 in the troposphere is anticipated in future climate scenarios (Collins et al., 2003; Sudo et al., 2003; Olsen et al., 2007).

6 Conclusions

In this paper, we compared the simulated long term trends in the daily maximum 8-h average summertime surface O_3 concentrations with observations in several sites in

ACPD
12, 2025–2056, 2012

Europe and the United States. The observed O_3 concentrations are decreasing at the high end of the probability distribution in the majority of the examined sites in both regions, related most probably to the decrease in local O_3 precursor emissions. The model overestimates this decrease, which may be related to an overestimated decline in the local emission inventories. In the model, the decrease in high O_3 levels is also in part related to changes in the meteorological conditions, without being able however to dismantle the exact reason.

At the low percentiles, observations show much larger variability in O_3 trends even between nearby sites. However, there is a marked change in the distribution, with the high (low) end, show decreasing (increasing) O_3 concentrations, respectively. The increase at the low O_3 levels is probably related to an increase in the background O_3 concentrations, which however is not captured in the model, except to a small extent at some sites in the western United States. This is a common feauture in most modeling studies, which show lesser increases in background ozone during the 1990s than observations suggest, as summarized by Logan et al. (2010). The reason of the difficulty of our model to represent the low percentile changes is related to its ability to reproduce (a) the long range transport events, the associated chemical processes, and possibly the magnitude of ozone precursor emissions and (b) the stratosphere-troposphere exchange.

Acknowledgements. This work was supported by funding from the Swiss National Science Foundation under grant 200020-112231 and from the Swiss Federal Office for the Environment. The GEOS-Chem model is managed by the Atmospheric Chemistry Modeling group at Harvard University with support of the NASA Atmospheric Chemistry Modeling and Analysis Program.In addition, we are grateful to the World Data Center for Greenhouse Gases, the European Monitoring and Evaluation Program, and the Clean Air Status and Trends Network for providing the different set of data used in this study.

ACPD
12, 2025–2056, 2012

References

Arino, O. and Melinotte, J. M.: Fire index atlas, Earth observation quaterly, 50, 11–16, 1995. 2030

Auvray, M. and Bey, I.: Long-range transport to Europe: Seasonal variations and implications for the European ozone budget, J. Geophys. Res.-Atmos., 110, 303–325, 2005. 2037

Benkovitz, C. M., Scholtz, M. T., Pacyna, J., Tarrason, L., Dignon, J., Voldner, E. C., Spiro, P. A., Logan, J. A., and Graedel, T. E.: Global gridded inventories of anthropogenic emissions of sulfur and nitrogen, J. Geophys. Res.-Atmos., 101, 29239–29253, 1996. 2028

Bey, I., Jacob, D. J., Logan, J. A., and Yantosca, R. M.: Asian chemical outflow to the Pacific in spring: Origins, pathways, and budgets, J. Geophys. Res.-Atmos., 106, 23097–23113, 2001a. 2028

Bey, I., Jacob, D. J., Yantosca, R. M., Logan, J. A., Field, B. D., Fiore, A. M., Li, Q. B., Liu, H. G. Y., Mickley, L. J., and Schultz, M. G.: Global modeling of tropospheric chemistry with assimilated meteorology: Model description and evaluation, J. Geophys. Res.-Atmos., 106, 23073–23095, 2001b. 2028

Bronnimann, S., Buchmann, B., and Wanner, H.: Trends in near-surface ozone concentrations in Switzerland: the 1990s, Atmos. Environ., 36, PII S1352–2310(02)00145–0, 2002. 2027

Collins, W. J., Derwent, R. G., Garnier, B., Johnson, C. E., Sanderson, M. G., and Stevenson, D. S.: Effect of stratosphere-troposphere exchange on the future tropospheric ozone trend, J. Geophys. Res.-Atmos., 108, 8528–8538, 2003. 2039

Cooper, O. R., Parrish, D. D., Stohl, A., Trainer, M., Nedelec, P., Thouret, V., Cammas, J. P., Oltmans, S. J., Johnson, B. J., Tarasick, D., Leblanc, T., McDermid, I. S., Jaffe, D., Gao, R., Stith, J., Ryerson, T., Aikin, K., Campos, T., Weinheimer, A., and Avery, M. A.: Increasing springtime ozone mixing ratios in the free troposphere over western North America, Nature, 463, 344–348, 2010. 2027

Cristofanelli, P. and Bonasoni, P.: Background ozone in the southern Europe and Mediterranean area: Influence of the transport processes, Environ. Pollut., 157, 1399–1406, 2009. 2033

Cui, J., Deolal, S. P., Sprenger, M., Henne, S., Staehelin, J., Steinbacher, M., and Nedelec, P.: Free tropospheric ozone changes over Europe as observed at Jungfraujoch (1990-2008): An analysis based on backward trajectories, J. Geophys. Res.-Atmos., 116, D10304, doi:10.1029/2010JD015154, 2011. 2033

Duncan, B. N., Martin, R. V., Staudt, A. C., Yevich, R., and Logan, J. A.: Interannual and

ACPD
12, 2025–2056, 2012

seasonal variability of biomass burning emissions constrained by satellite observations, J. Geophys. Res.-Atmos., 108, 4100–4122, 2003. 2030

Duncan, B. N., Logan, J. A., Megretskaia, I. A., Yantosca, R. M., Novelli, P. C., Jones, N. B., and Rinsland, C. P.: The global budget of CO, 1988-1997: source estimates and validation with a global model, J. Geophys. Res.-Atmos., 112, D22301, doi:10.1029/2007JD008459, 2007. 2028

EEA: Annual European Community LRTAP Convention Emission inventory report 1990-2005 (2007), Technical report No 14/2007 (available at: http://reports.eea.europa.eu/technical_report_2007_14/en/Tech_report_14_2007_AnnualEC_LRTAP.pdf)., Tech. rep., European Environment Agency, Denmark, 2007. 2035

EMEP: Fjaeraa, A. M., and A-G. Hjellbrekke, Ozone measurements 2006, EMEP/CCC-Report 2/2008, 0-7727, April 2008, (available at: http://www.nilu.no/projects/ccc/reports/cccr4-2008.pdf)., Tech. rep., Norwegian Meteorological institute, Norway, 2008. 2027

EPA: Cuideline on data handling conventions for the 8-hour ozone NAAQS, Tech. rep., US Environmental Protection Agency, Research Triangle Park, North Carolina, 1998. 2031

EPA: National air pollutant emission trends, 1990–1998, Rep. EPA-454/R-00-002, Tech. rep., US Environmental Protection Agency, Research Triangle Park, N.C., 2000. 2029

EPA: Latest Findings on National air quality – Status and Trends through 2006 (available at: http://www.epa.gov/air/airtrends/2007/)., EPA-454/R-07-007, Tech. rep., US Environmental Protection Agency, Research Triangle Park, North Carolina, 2007. 2027, 2029

Fiore, A. M., Jacob, D. J., Bey, I., Yantosca, R. M., Field, B. D., Fusco, A. C., and Wilkinson, J. G.: Background ozone over the United States in summer: Origin, trend, and contribution to pollution episodes, J. Geophys. Res.-Atmos., 107, 4275–4300, 2002. 2037

Fiore, A. M., Dentener, F. J., Wild, O., Cuvelier, C., Schultz, M. G., Hess, P., Textor, C., Schulz, M., Doherty, R. M., Horowitz, L. W., MacKenzie, I. A., Sanderson, M. G., Shindell, D. T., Stevenson, D. S., Szopa, S., Van Dingenen, R., Zeng, G., Atherton, C., Bergmann, D., Bey, I., Carmichael, G., Collins, W. J., Duncan, B. N., Faluvegi, G., Folberth, G., Gauss, M., Gong, S., Hauglustaine, D., Holloway, T., Isaksen, I. S. A., Jacob, D. J., Jonson, J. E., Kaminski, J. W., Keating, T. J., Lupu, A., Marmer, E., Montanaro, V., Park, R. J., Pitari, G., Pringle, K. J., Pyle, J. A., Schroeder, S., Vivanco, M. G., Wind, P., Wojcik, G., Wu, S., and Zuber, A.: Multimodel estimates of intercontinental source-receptor relationships for ozone pollution, J. Geophys. Res.-Atmos., 114, 114, D04301, doi:10.1029/2008JD010816, 2009. 2037

Frost, G. J., McKeen, S. A., Trainer, M., Ryerson, T. B., Neuman, J. A., Roberts, J. M., Swanson,

ACPD
12, 2025–2056, 2012

A., Holloway, J. S., Sueper, D. T., Fortin, T., Parrish, D. D., Fehsenfeld, F. C., Flocke, F., Peckham, S. E., Grell, G. A., Kowal, D., Cartwright, J., Auerbach, N., and Habermann, T.: Effects of changing power plant NO_x emissions on ozone in the eastern United States: Proof of concept, J. Geophys. Res.-Atmos., 111, D12306, doi:10.1029/2005JD006354, 306, 2006. 2036

Generoso, S., Bréon, F.-M., Balkanski, Y., Boucher, O., and Schulz, M.: Improving the seasonal cycle and interannual variations of biomass burning aerosol sources, Atmos. Chem. Phys., 3, 1211–1222, doi:10.5194/acp-3-1211-2003, 2003. 2030

Herman, J. R., Bhartia, P. K., Torres, O., Hsu, C., Seftor, C., and Celarier, E.: Global distribution of UV-absorbing aerosols from Nimbus 7/TOMS data, J. Geophys. Res.-Atmos., 102, 16911–16922, 1997. 2030

Hogrefe, C., Hao, W., Zalewsky, E. E., Ku, J.-Y., Lynn, B., Rosenzweig, C., Schultz, M. G., Rast, S., Newchurch, M. J., Wang, L., Kinney, P. L., and Sistla, G.: An analysis of long-term regional-scale ozone simulations over the Northeastern United States: variability and trends, Atmos. Chem. Phys., 11, 567–582, doi:10.5194/acp-11-567-2011, 2011. 2035

Hsu, N. C., Herman, J. R., Bhartia, P. K., Seftor, C. J., Torres, O., Thompson, A. M., Gleason, J. F., Eck, T. F., and Holben, B. N.: Detection of biomass burning smoke from TOMS measurements, Geophys. Res. Lett., 23, 745–748, 1996. 2030

Hudman, R. C., Jacob, D. J., Cooper, O. R., Evans, M. J., Heald, C. L., Park, R. J., Fehsenfeld, F., Flocke, F., Holloway, J., Hubler, G., Kita, K., Koike, M., Kondo, Y., Neuman, A., Nowak, J., Oltmans, S., Parrish, D., Roberts, J. M., and Ryerson, T.: Ozone production in transpacific Asian pollution plumes and implications for ozone air quality in California, J. Geophys. Res.-Atmos., 109, D23S10, doi:10.1029/2004JD004974, 2004. 2039

Hudman, R. C., Jacob, D. J., Turquety, S., Leibensperger, E. M., Murray, L. T., Wu, S., Gilliland, A. B., Avery, M., Bertram, T. H., Brune, W., Cohen, R. C., Dibb, J. E., Flocke, F. M., Fried, A., Holloway, J., Neuman, J. A., Orville, R., Perring, A., Ren, X., Sachse, G. W., Singh, H. B., Swanson, A., and Wooldridge, P. J.: Surface and lightning sources of nitrogen oxides over the United States: Magnitudes, chemical evolution, and outflow, J. Geophy. Res.-Atmos., 112, D12S05, doi:10.1029/2006JD007912, 2007. 2029

IPCC: Aviation and the global atmosphere Joyce E. Penner, David H. Lister, David J. Griggs , David J. Dokken, Mack McFarland, Tech. rep., 1999. 2029

IPCC: Summary for Policymakers. in: Climate Change 2007: The Physical Science Basis. Contribution of Working Group I to the Fourth Assessment Report of the Intergovernmental

ACPD
12, 2025–2056, 2012

Panel on Climate Change, edited by: Solomon, S., Qin, D., Manning, M., Chen, Z., Marquis, M., Averyt, K. B., Tignor, M., and Miller, H. L., Tech. rep., 2007. 2026

Jaffe, D., Price, H., Parrish, D., Goldstein, A., and Harris, J.: Increasing background ozone during spring on the west coast of North America, Geophys. Res. Lett., 30, 1613–1617, 2003. 2037

Jonson, J. E., Simpson, D., Fagerli, H., and Solberg, S.: Can we explain the trends in European ozone levels?, Atmos. Chem. Phys., 6, 51–66, doi:10.5194/acp-6-51-2006, 2006. 2027, 2029, 2033

Kim, S. W., Heckel, A., McKeen, S. A., Frost, G. J., Hsie, E. Y., Trainer, M. K., Richter, A., Burrows, J. P., Peckham, S. E., and Grell, G. A.: Satellite-observed US power plant NO_x emission reductions and their impact on air quality, Geophys. Res. Lett., 33, 812, 2006. 2036

Koumoutsaris, S., Bey, I., Generoso, S., and Thouret, V.: Influence of El Niño-Southern Oscillation on the interannual variability of tropospheric ozone in the northern midlatitudes, Journal Of Geophysical Research-Atmospheres, 113, 2008. 2027, 2028, 2030, 2031, 2032, 2039

Kurokawa, J.-i., Yumimoto, K., Uno, I., and Ohara, T.: Adjoint inverse modeling of NO(x) emissions over eastern China using satellite observations of NO(2) vertical column densities, Atmos. Environ., 43, 1878–1887, 2009. 2038

Liang, Q., Jaegle, L., Hudman, R. C., Turquety, S., Jacob, D. J., Avery, M. A., Browell, E. V., Sachse, G. W., Blake, D. R., Brune, W., Ren, X., Cohen, R. C., Dibb, J. E., Fried, A., Fuelberg, H., Porter, M., Heikes, B. G., Huey, G., Singh, H. B., and Wennberg, P. O.: Summertime influence of Asian pollution in the free troposphere over North America, Journal of Geophysical Research-Atmospheres, 112, D12S11, 2007. 2037, 2038, 2039

Lin, C. Y. C., Jacob, D. J., Munger, J. W., and Fiore, A. M.: Increasing background ozone in surface air over the United States, Geophysical Research Letters, 27, 3465–3468, 2000. 2026, 2027, 2031, 2034, 2037

Liu, H. Y., Jacob, D. J., Bey, I., Yantosca, R. M., Duncan, B. N., and Sachse, G. W.: Transport pathways for Asian pollution outflow over the Pacific: interannual and seasonal variations, Journal of Geophysical Research-Atmospheres, 108, 8786, 2003. 2037

Lobert, J. M., Keene, W. C., Logan, J. A., and Yevich, R.: Global chlorine emissions from biomass burning: Reactive Chlorine Emissions inventory, J. Geophys. Res.-Atmos., 104, 8373–8389, 1999. 2030

Logan, J. A., Schultz, M., and Oltmans, S.: Observing and Understanding Tropo-

ACPD
12, 2025–2056, 2012

spheric Ozone Changes, EOS Transactions American Geophysical Union, 91, 119, doi:10.1029/2010EO130004, 2010. 2032, 2040
Naja, M., Akimoto, H., and Staehelin, J.: Ozone in background and photochemically aged air over central Europe: Analysis of long-term ozonesonde data from Hohenpeissenberg and Payerne, J. Geophys. Res.-Atmo., 108, 4063–4074, 2003. 2037
Ohara, T., Akimoto, H., Kurokawa, J., Horii, N., Yamaji, K., Yan, X., and Hayasaka, T.: An Asian emission inventory of anthropogenic emission sources for the period 19802020, Atmos. Chem. Phys., 7, 4419–4444, doi:10.5194/acp-7-4419-2007, 2007. 2029
Ohara, T., Yamaji, K., Uno, I., Tanimoto, H., Sugata, S., Nagashima, T., Kurokawa, J. I., Horii, N., and Alkimoto, H.: Long-term simulations of surface ozone in east Asia during 1980-2020 with CMAQ and REAS inventory, Air Pollution Modeling And Its Application Xix, 136–144, 2008. 2037
Olsen, M. A., Schoeberl, M. R., and Nielsen, J. E.: Response of stratospheric circulation and stratosphere-troposphere exchange to changing sea surface temperatures, J. Geophys. Res.-Atmos., 112, D16104, doi:10.1029/2006JD008012, 2007. 2039
Oltmans, S. J., Lefohn, A. S., Harris, J. M., Galbally, I., Scheel, H. E., Bodeker, G., Brunke, E., Claude, H., Tarasick, D., Johnson, B. J., Simmonds, P., Shadwick, D., Anlauf, K., Hayden, K., Schmidlin, F., Fujimoto, T., Akagi, K., Meyer, C., Nichol, S., Davies, J., Redondas, A., and Cuevas, E.: Long-term changes in tropospheric ozone, Atmos. Environ., 40, 3156–3173, 2006. 2026, 2027
Ordóñez, C., Brunner, D., Staehelin, J., Hadjinicolaou, P., Pyle, J. A., Jonas, M., Wernli, H., and Prevot, A. S. H.: Strong influence of lowermost stratospheric ozone on lower tropospheric background ozone changes over Europe, Geophys. Res. Lett., 34, L07805, doi:10.1029/2006GL029113, 2007. 2037, 2039
Piccot, S. D., Watson, J. J., and Jones, J. W.: A global inventory of volatile organic-compound emissions from anthropogenic sources, J. Geophys. Res.-Atmos., 97, 9897–9912, 1992. 2028
Pickering, K. E., Wang, Y. S., Tao, W. K., Price, C., and Müller, J. F.: Vertical distributions of lightning NO_x for use in regional and global chemical transport models, J. Geophys. Res.-Atmos., 103, 31203–31216, 1998. 2030
Price, C. and Rind, D.: A simple lightning parameterization for calculating global lightning distributions, J. Geophys. Res.-Atmos., 97, 9919–9933, 1992. 2030
Schär, C., Vidale, P. L., Luthi, D., Frei, C., Haberli, C., Liniger, M. A., and Appenzeller, C.:

ACPD
12, 2025–2056, 2012

The role of increasing temperature variability in European summer heatwaves, Nature, 427, 332–336, 2004. 2031

Sillman, S. and He, D. Y.: Some theoretical results concerning O3-NOx-VOC chemistry and NOx-VOC indicators, J. Geophys. Res.-Atmos., 107, 4659–4674, 2002. 2034

Simpson, D.: Biogenic emissions in Europe 2. Implications For Ozone Control Strategies, J. Geophys. Res.-Atmos., 100, 22891–22906, 1995. 2033

Staehelin, J. and Weiss, A. K.: Swiss history of atmospheric ozone research and results of long-term Swiss ozone measurements, Ozone-Sci. Eng., 23, 461–466, 2001. 2026

Sudo, K., Takahashi, M., and Akimoto, H.: Future changes in stratosphere-troposphere exchange and their impacts on future tropospheric ozone simulations, Geophys. Res. Lett., Geophys. Res. Lett., 30, 2256, doi:10.1029/2003GL018526, 2003. 2039

Tarasova, O. A., Senik, I. A., Sosonkin, M. G., Cui, J., Staehelin, J., and Prévôt, A. S. H.: Surface ozone at the Caucasian site Kislovodsk High Mountain Station and the Swiss Alpine site Jungfraujoch: data analysis and trends (19902006), Atmos. Chem. Phys., 9, 4157–4175, doi:10.5194/acp-9-4157-2009, 2009. 2039

Torres, O., Bhartia, P. K., Herman, J. R., Ahmad, Z., and Gleason, J.: Derivation of aerosol properties from satellite measurements of backscattered ultraviolet radiation: Theoretical basis, J. Geophys. Res.-Atmos., 103, 17099–17110, 1998. 2030

Uno, I., He, Y., Ohara, T., Yamaji, K., Kurokawa, J.-I., Katayama, M., Wang, Z., Noguchi, K., Hayashida, S., Richter, A., and Burrows, J. P.: Systematic analysis of interannual and seasonal variations of model-simulated tropospheric NO2 in Asia and comparison with GOME-satellite data, Atmos. Chem. Phys., 7, 1671–1681, doi:10.5194/acp-7-1671-2007, 2007. 2038

Vestreng, V., Rigler, E., Adams, M., Kindbom, K., Pacyna, J. M., Denier van der Gon, H., Reis, S., and Travnikov, O.: Inventory review 2006, Emission data reported to LRTAP and NEC Directive, Stage 1, 2 and 3 review and Evaluation of Inventories of HM and POPs. EMEP/MSC-W Technical Report 1/2006 ISSN 1504-6179, available at: http://www.emep.int/, Tech. rep., EMEP/MSC-Wy, 2006. 2028

Vingarzan, R.: A review of surface ozone background levels and trends, Atmos. Environ., 38, 3431–3442, 2004. 2026, 2027, 2034

Wang, Y. H., Jacob, D. J., and Logan, J. A.: Global simulation of tropospheric O_3-NO_x-hydrocarbon chemistry 1. Model formulation, J. Geophys. Res.-Atmos., 103, 10713–10725, 1998a. 2029

ACPD

12, 2025–2056, 2012

Wang, Y. H., Logan, J. A., and Jacob, D. J.: Global simulation of tropospheric O_3-NO_x-hydrocarbon chemistry 2. Model evaluation and global ozone budget, J. Geophys. Res.-Atmos., 103, 10727–10755, 1998b. 2028, 2030

WMO: WMO WDCGG DATA SUMMARY, WDCGG No.32, GAW data, Volume IV-Grennhouse gases and Other Atmospheric Gases, Published by Japan Meteorological Agency in co-operation with World Meteorological Organisation, (available at: http://gaw.kishou.go.jp/wdcgg/products/summary/sum32/sum32contents.html)., Tech. rep., World Meteorological Organization, Geneva, Switzerland., 2008. 2027

Xu, X., Lin, W., Wang, T., Yan, P., Tang, J., Meng, Z., and Wang, Y.: Long-term trend of surface ozone at a regional background station in eastern China 19912006: enhanced variability, Atmos. Chem. Phys., 8, 2595–2607, doi:10.5194/acp-8-2595-2008, 2008. 2037

Yienger, J. J. and Levy, H.: Empirical-model of global soil-biogenic NO_x emissions, J. Geophys. Res.-Atmos., 100, 11447–11464, 1995. 2029

Zellweger, C., Ammann, M., Buchmann, B., Hofer, P., Lugauer, M., Ruttimann, R., Streit, N., Weingartner, E., and Baltensperger, U.: Summertime NOy speciation at the Jungfraujoch, 3580 m above sea level, Switzerland, J. Geophys. Res.-Atmos., 105, 6655–6667, 2000. 2033

Zhang, L., Jacob, D. J., Boersma, K. F., Jaffe, D. A., Olson, J. R., Bowman, K. W., Worden, J. R., Thompson, A. M., Avery, M. A., Cohen, R. C., Dibb, J. E., Flock, F. M., Fuelberg, H. E., Huey, L. G., McMillan, W. W., Singh, H. B., and Weinheimer, A. J.: Transpacific transport of ozone pollution and the effect of recent Asian emission increases on air quality in North America: an integrated analysis using satellite, aircraft, ozonesonde, and surface observations, Atmos. Chem. Phys., 8, 6117–6136, doi:10.5194/acp-8-6117-2008, 2008. 2038

ACPD
12, 2025–2056, 2012

Table 1. Simulations performed with the GEOS-Chem model in the present work.

Name	Period	Configuration
Control simulation		
S0	1991–2005	All parameters vary interannually
Sensitivity simulations		
SEur	2001–2005	European anthropogenic emissions fixed in 1990
SNam	2001–2005	North American anthropogenic emissions fixed in 1990
SSAs	2001–2005	South Asian anthropogenic emissions fixed in 1990
SEAs	2001–2005	East Asian anthropogenic emissions fixed in 1990
SXEur	2001–2005	North American, East and South Asian anthropogenic emissions fixed in 1990. and Methane concentrations fixed in 1990.
SMET	2001–2005	Meteorology of 10 years before (i.e. 1991–1995)

ACPD
12, 2025–2056, 2012

Table 2. Model performance metrics for the daily maximum 8-h average summer O_3 concentration at all available sites for 1991–2005 for 5 percentiles. Column a: the three numbers correspond to the number of sites with correlation coefficient lower or equal to 0.3, between 0.3 and 0.7, and greater than or equal to 0.7, respectively. Column b: The mean bias is calculated for 5 percentiles for each site and then averaged to display in this table. Results are shown separately for sites in Europe and US.

Percentile	(a) $R \leq 0.3$, $0.3 < R < 0.7$, $R \geq 0.7$	(b) Mean bias, ppb (%)
Europe – 44 sites		
5th	21, 21, 2	−7.3 (−21.2 %)
20th	14, 20, 10	−2.7 (−10.3 %)
50th	4, 27, 13	−0.9 (−4.3 %)
80th	3, 17, 24	1.6 (0.6 %)
95th	2, 17, 25	5.6 (6.5 %)
USA – 38 sites		
5th	21, 15, 2	−16.1 (−66.2 %)
20th	5, 13, 20	−15.0 (−36.2 %)
50th	1, 13, 24	−13.9 (−26.9 %)
80th	0, 10, 28	−10.9 (−17.4 %)
95th	4, 25, 9	−2.4 (−2.4 %)

ACPD
12, 2025–2056, 2012

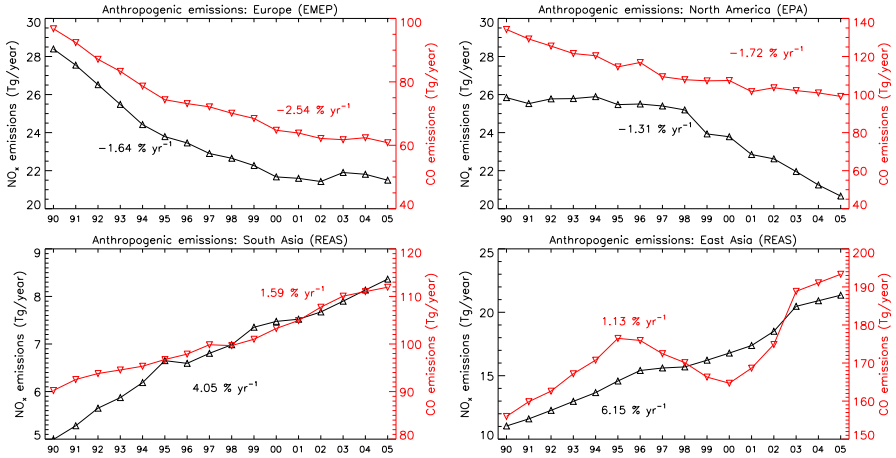

Fig. 1. Interannual (from 1990 to 2005) anthropogenic emissions of NO_x (in black) and CO (in red) implemented in the GEOS-Chem model over four important anthropogenic source regions: North America, South Asia, Europe, and East Asia.

ACPD
12, 2025–2056, 2012

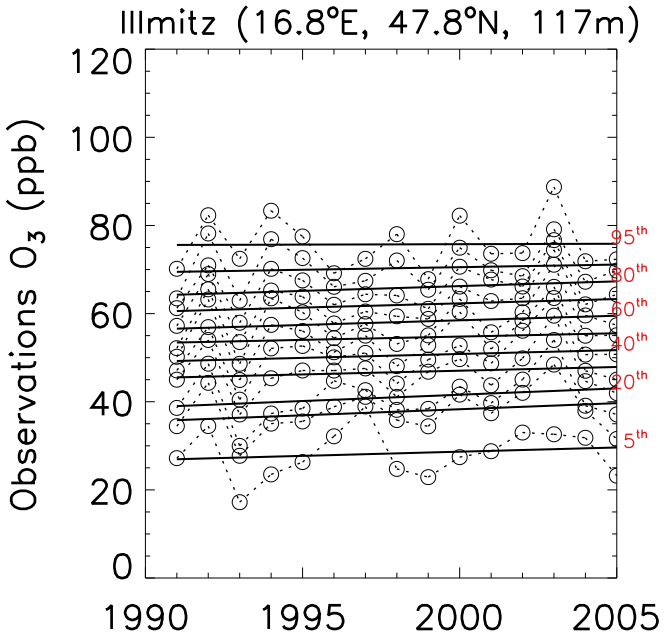

Fig. 2. Observed interannual (from 1990 to 2005) variation (dotted lines) and linear trends (solid lines) in several percentile populations of the summertime O_3 concentrations for the station of Illmitz, in Austria.

ACPD
12, 2025–2056, 2012

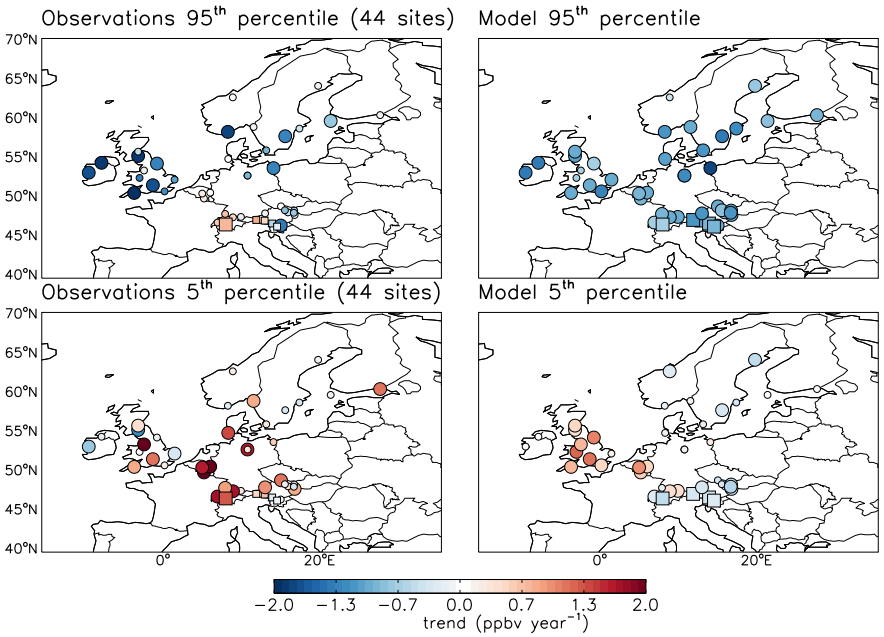

Fig. 3. Trends (% year^{-1}) in the 95th (top) and 5th (bottom) percentile of the distribution of the 8-hour daily maximum summertime O_3 concentrations at 44 European stations for the observations (left) and the model (right). The simulated trends (right panels) are computed using the hourly model O_3 values from the control simulation ("S0"). Circles and squares denote trends at sites above and below 1500 m, respectively. Large symbols denote significant trends at the 0.05 level. Small symbols denote trends that are not statistically significant.

ACPD
12, 2025–2056, 2012

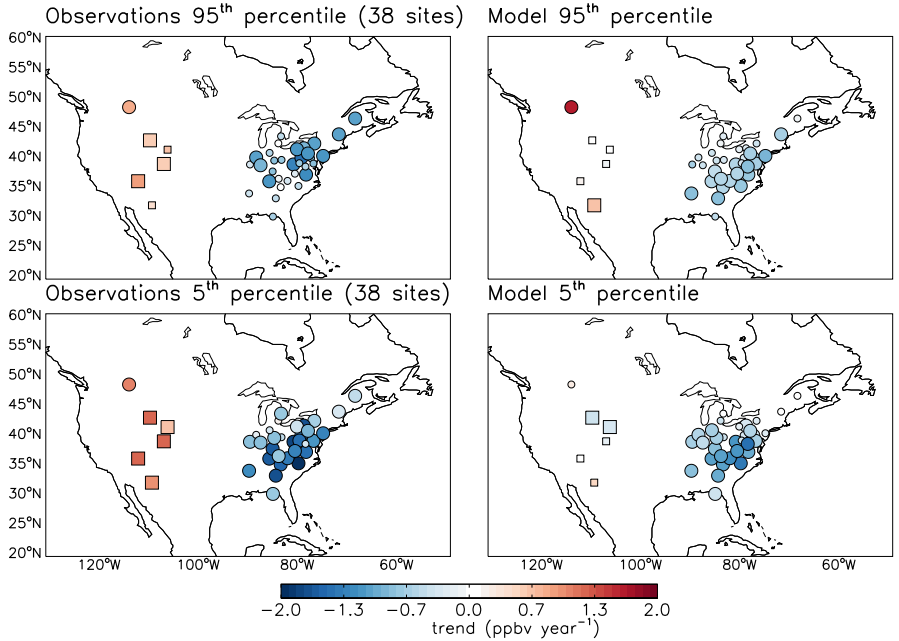

Fig. 4. Trends (% year^{-1}) in the 95th (top) and 5th (bottom) percentile of the distribution of the 8-h daily maximum summertime O_3 concentrations at 38 US stations for the observations (left) and the model (right). Circles and squares denote trends at sites above and below 1500 m, respectively. Large symbols denote significant trends at the 0.05 level. Small symbols denote trends that are not statistically significant.

ACPD
12, 2025–2056, 2012

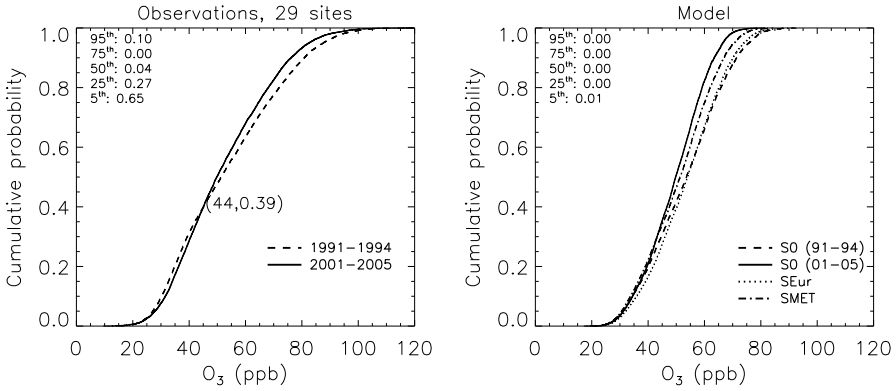

Fig. 5. Cumulative probability distribution of the 8-h daily maximum summertime (JJA) O_3 concentrations at rural sites in Europe in 1991–1994 (dashed line) and 2001–2005 (solid line). We exclude the anomalous hot year 2003 and also the sites with titration effects (see Sect. 4.1.1 for details). The statistical significance level between the two distributions (1991–1994 vs. 2001–2005) is indicated for 5 percentiles in the upper left corner of each panel. The sensitivity simulations "SEur" (dotted line) and "SMet" (slash-dot line) are significantly different from "S0".

ACPD
12, 2025–2056, 2012

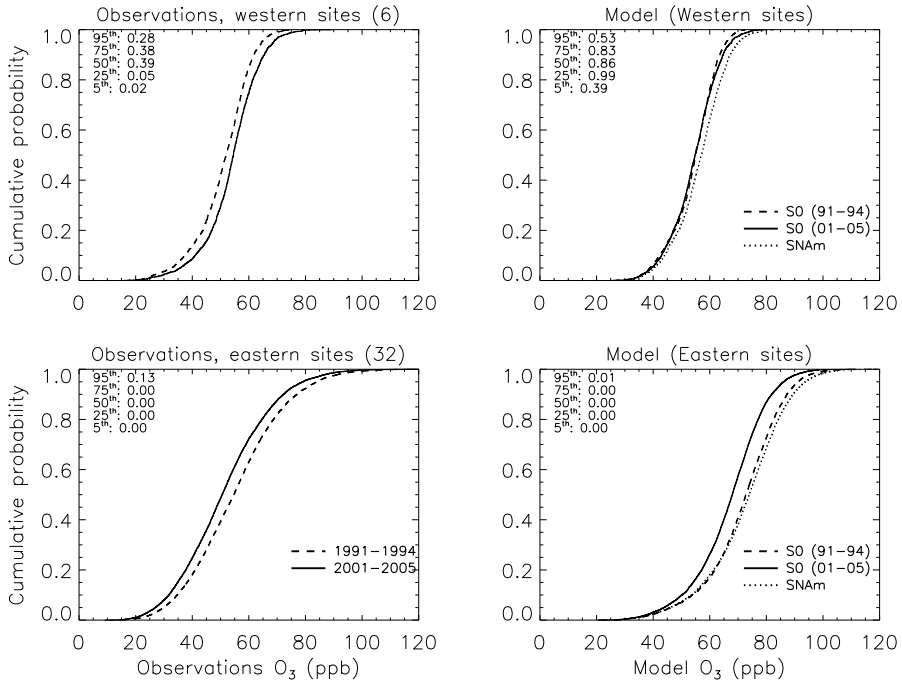

Fig. 6. Cumulative probability distribution of the 8-hour daily maximum summertime (JJA) O_3 concentrations at rural sites in the US in 1991–1994 (dashed line) and 2001–2005 (solid line). For consistency with Europe, we exclude the year 2003. Bottom panels: western US sites. Top panels: eastern US sites (see text for details). Observations and model results are shown in the left and right panels, respectively. The statistical significance level between the two distributions (1991–1994 vs. 2001–2005) is indicated for 5 percentiles in the upper left corner of each panel. The sensitivity simulation "SNAm" (dotted line) is significantly different from "S0" (period 2001–2005, see also SOM).

ACPD
12, 2025–2056, 2012

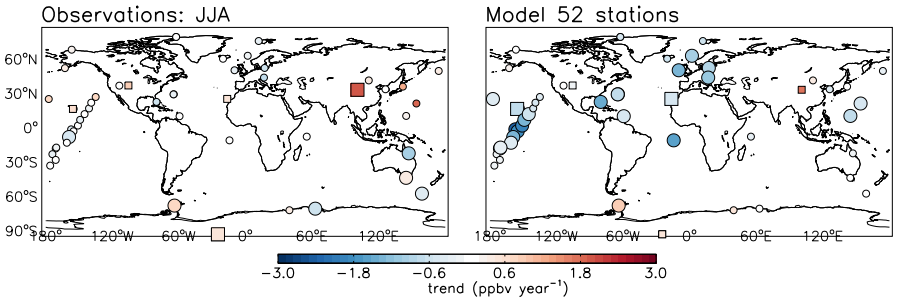

Fig. 7. Trends (% year^{-1}) in the summertime CO concentrations at 52 stations from the WDCGG network for the observations (left) and the model (right). Circles and squares denote trends at sites above and below 1500 m, respectively. Large symbols denote significant trends at the 0.05 level. Small symbols denote trends that are not statistically significant.

ACPD
12, 2025–2056, 2012